Journal of Materials Chemistry B

Accepted Manuscript

ROYAL SOCIETY OF CHEMISTRY

www.rsc.org/materialsB

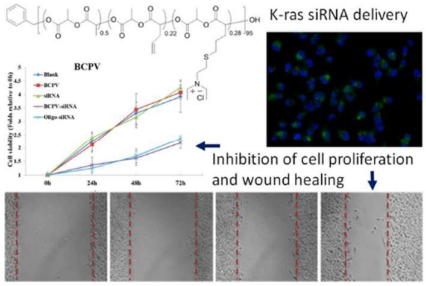

Biodegradable nanoparticles mediated K-ras siRNA delivery has shown inhibition of cell proliferation, migration and invasion in pancreatic cancer cells.

Journal of Materials Chemistry B

RSCPublishing

ARTICLE

Biodegradable nanoparticle-mediated K-ras down regulation for pancreatic cancer gene therapy

Cite this: DOI: 10.1039/x0xx00000x

Received 00th January 2012,
Accepted 00th January 2012

DOI: 10.1039/x0xx00000x

www.rsc.org/

Chengbin Yang[a], Rui Hu[a], Tommy Anderson[a], Yucheng Wang[a], Guimiao Lin[b], Wing-Cheung Law[c], Wei-Jen Lin[d], Quoc Toan Nguyen[e], Hui Ting Toh[e], Ho Sup Yoon[e], Chih-Kuang Chen[d*], and Ken-Tye Yong[a*]

[a]School of Electrical and Electronic Engineering, Nanyang Technological University, Singapore 639798, Singapore
[b]The Engineering Lab of Synthetic Biology and the Key Lab of Biomedical Engineering, School of Medicine, Shenzhen University, Shenzhen, 518060, China
[c]Department of Industrial and Systems Engineering, The Hong Kong Polytechnic University, Hung Hom, Kowloon, Hong Kong, P.R. China
[d]The Polymeric Biomaterials Lab, Department of Fiber and Composite Materials, Feng Chia University, Taichung, Taiwan 40724, ROC
[e]Division of Structural Biology & Biochemistry, School of Biological Sciences, Nanyang Technological University, Singapore 639798, Singapore

*Corresponding authors:
Chih-Kuang Chen, PhD, The Polymeric Biomaterials Lab, Department of Fiber and Composite Materials, Feng Chia University, Taichung, Taiwan 40724, ROC, Tel: +886-4-24517250 ext.3444, email: chihkuan@mail.fcu.edu.tw
Ken-Tye Yong, PhD, School of Electrical and Electronic Engineering, Nanyang Technological University, Singapore 639798, Singapore Tel: +65-6790-5444, email: ktyong@ntu.edu.sg

Abstract. RNA interference (RNAi) targeting the K-ras oncogene mutation in pancreatic cancer mediated by small interfering RNA (siRNA) transfection is a very promising treatment. However, the rapid degradation and negative charge of naked siRNAs restrict the direct delivery of them into cells. In this contribution, we propose a safe and effective transmembrane transport nanocarrier formulation based on a newly developed biodegradable charged polyester-based vector (BCPV) for K-ras siRNA delivery into pancreatic cancer cells. Our results have shown that these biodegradable and biocompatible vectors are able to transfect mutant K-ras siRNAs into the MiaPaCa-2 cells with high transfection and knockdown efficiency. More importantly, the RNAi process has initiated a cascade gene regulation of the downstream proteins of K-ras associated with cell proliferation, migration, invasion and apoptosis. We observed that after the mutant K-ras siRNA transfection, the growth, migration and invasion of MiaPaCa-2 cells have been significantly reduced; the apoptosis of the pancreatic cancer cells has also been promoted. Although in vivo testing data are limited, we propose that the BCPV based nanoparticle formulation could be a promising candidate as non-viral vectors for gene therapy in clinical settings.

Key words: pancreatic cancer, siRNA, BCPV, K-ras, cell apoptosis

1. Introduction

Pancreatic cancer is listed as the fourth leading cause of cancer related death, yet its prognosis has not been improved over the past 40 years[1]. In lack of specific early symptoms and early detection methods, it is usually diagnosed at advanced and incurable stage[2] and usually result in fatal come even after treatment with existing therapies[3]. Gene sequencing analysis revealed that K-ras mutations are very common genetic mutations which rates approximately 90% in pancreatic cancers and occurs mostly in the early stages of pancreatic cell transformations and tumor progression[4]. The activated K-ras oncoproteins are thought to alter the cellular signal transduction pathways and enhance the neoplastic growth of the

pancreatic cancers[5, 6]. Reports have shown that the down regulated K-ras gene expression causes reduced proliferation and migration, and increase of apoptosis in MiaPaCa-2 cells[7]. Therefore, the mutant K-ras gene transcripts can be used as potential targets of specific gene modulation for suppressing the development of the pancreatic cancer.

Among gene therapy strategies, RNA interference (RNAi) has received great interests in the past decade. RNAi is a process of post-transcriptional gene silencing where a sequence specific double-stranded RNA is introduced to trigger the degradation of the targeted messenger RNA (mRNA) homologous[8]. It can be initiated by endogenous microRNAs (miRNAs) or synthetic small interfering RNAs (siRNAs), of which the latter mimics the structure of Dicer products and is incorporated in the pathway downstream of the Dicer enzyme[9]. When delivered into the cytoplasm, siRNAs are incorporated into a nuclease complex, which then identifies and binds to the target mRNA[10]. Consequently the bound mRNA is rapidly degraded and interrupted from being translated into protein[11-14]. In recent years, siRNAs have been widely used for targeted gene silencing in pancreatic cancer therapy. For example, siRNA targeting HIF-1α suppressed pancreatic cancer cell proliferation and induced cell apoptosis[15]. Zhi et al. have used siRNAs against matrix metalloproteinase-2 (MMP-2) to decrease the pancreatic cancer cell adhesion and invasion[16]. Another study has demonstrated that the silencing of sphingosine kinase-1 can sensitize the pancreatic cancer cells to chemotherapy drugs[17]. All these results have shown great promises towards a breakthrough of pancreatic cancer therapy.

Although RNAi initiated by siRNAs has great potentials for gene therapy, the application of siRNA faces a series of challenges. Naked siRNAs are not stable due to nuclease-mediated degradation and they are negatively charged. Without proper carriers, they cannot enter a cell by itself. On the other hand, the carriers need to be nontoxic and able to deliver siRNA with high efficiency. Most importantly, the carriers should be able to efficiently release the siRNAs so that they can interact with the RNAi machinery[18]. Furthermore, naked siRNAs are possibly immunogenic in the bloodstream and not able to cross biological barriers to reach the lesion site[19]. Viral vectors have been considered as a promising candidate because of their high gene transfection efficiency. However, due to the size limitation of the inserted genetic materials, the possible immune response and the biosafety risk, the application of viral vectors has been restricted[20]. Non-viral vectors have thus been greatly investigated, such as lipids, polymers, peptides, antibodies, aptamers, nanoparticles and small molecules[9, 21-23]. Of these vectors, although some show promising results, their applications are often limited by low transfection efficiency and/or cytotoxicity. For example, cationic lipid complexes, which have been the most widely used carrier for delivery of siRNA[22], may cause severe membrane damages, reduced number of mitoses, cell shrinking and vacuolization of the cytoplasm[24].

In our previous work, the cationic polylactides, which can be referred to as biodegradable charged polyester-based vectors (BCPVs) have shown great promise as nanocarriers for siRNAs. Their high complexation ability and well-defined structure have led to the application for the delivery of siRNAs to prostate and pancreatic cancer cells[25]. More importantly, BCPV also exhibited very low toxicity, high biocompatibility and considerable hydrolytic degradability. To further advance the applicability of BCPV for gene delivery in clinical settings, transfection conditions need to be carefully optimized. The physiological characteristics of cancer cells are also important before preclinical animal experiments. In this study, we have optimized the BCPV-siRNA formulation for efficient delivery of mutant K-ras siRNAs into a pancreatic cancer cell line named MiaPaCa-2. After the gene silencing, we have carefully characterized the change in the cell proliferation and the metastasis indicators such as the cell migration and invasion in MiaPaCa-2 cells. Moreover, the mutant K-ras gene silencing has caused apparent apoptosis of MiaPaCa-2 cells. All these results suggest that the BCPV based nanoparticle formulation has a bright prospect as non-viral vectors for clinical cancer gene therapy.

2. Material and Methods

2.1. Synthesis of BCPVs and Characterization of Polyplexes

The BCPV was synthesized in accordance with the method reported previously[26]. The resulting vectors were characterized by ^{1}H-NMR and GPC, and their structural properties were reported as the followings: M_n^{NMR}=19.3 kDa; charge density: 28%; PDI^{GPC}=1.38. Hydrodynamic size and Zeta-potential of BCPV/siRNA polyplexes with different weight ratios were measured by Brookhaven 90Plus Particle Size Analyzer. Agarose gel retardation assays were utilized to determine the optimized dosage of BCPV required to interact completely with siRNA. SiRNA was mixed by gentle vortexing with BCPV at various ratio. After 20 minutes incubation at room temperature, the complex were loaded on a 1.2% agarose gel and electrophoresed at 100V for 15 minutes. Gels were observed under UV transilluminator (Bio-Rad).

2.2. Cell Culture

The human pancreatic cancer cells, MiaPaCa-2 (CRL-1420) obtained from American Type Culture Collection, which were used for this study, was maintained in culture with Dulbecco's Modified Eagle's Medium (DMEM, Hyclone), supplemented with 10% fetal bovine serum (FBS, Hyclone), 100units/mL penicillin (Gibco) and 100 μg/mL streptomycin (Gibco). Cells were cultured at 37 ℃ in a humidified atmosphere with 5% CO_2, and maintained as described previously[27].

2.3. Cytotoxicity

MiaPaCa-2 cells were seeded at 5×10^3 per well into 96-well plates and allowed to adhere for 24h. Cells were treated with different concentrations of Complex for 24 or 48 hours. Cell viability was measured by the MTT (3-(4, 5-Dimethylthiazol-2-yl)-2,5-diphenyltetrazolium bromide) (Sigma) assay kit as previously described[27]. The cell viability was obtained by normalizing the absorbance of the sample well against that from the control well and expressed as a percentage, assigning the viability of non-treated cells as 100%.

2.4. Transfection

The cells (1×10^4) were seeded onto 6-well plates in DMEM medium without antibiotics to give 30%-50% confluence at the time of transfections. BCPV (1mg/ml) dispersion was mixed with 20μL of 10μM K-Ras siRNA^{FAM} (Sense: 5'-FAM-GUUGGAGCUUGUGGCGUAGUU-3; Antisense: 5-CUACGCCACAAGCUCCAACUU-3,) with gentle vortex and incubated for 20 minutes. Before transfection, the culture medium was replaced with OPTI-MEM (Invitrogen), the above mentioned BCPV-siRNA^{FAM} mixture was then added to the 6-well plate wells and the cells were continuously cultured for four hours. After that, parts of cells were prepared for imaging under Inverted fluorescence microscope and transfection efficiency detecting by flow cytometry. The remaining cells in the dish were continue cultured with adding 500 μL DMEM medium with 30% FBS. Free siRNA^{FAM} was also used in another parallel experiment at the same dosage level. A commercial transfection reagent Oligofectamine™ (Invitrogen) coupled siRNA^{FAM} was used as positive control. The gene expression was monitored at 48 hours post-transfection. For transfection efficiency examination, fluorescence image were performed at 4 hours post-treatment.

2.5. Fluorescence imaging

In vitro fluorescence microscopy images were obtained using fluorescence microscope (Eclipse-Ti, Nikon). After 4h of incubation, the transfected cells were washed twice with PBS, and fixed with 4% formaldehyde. The cells were incubated with DAPI (Sigma) for nuclear counterstaining before performing the imaging experiments. To image the cells, filter sets for DAPI (excitation at 405 nm and emission was collected with a band pass filter 450/50 nm) and FITC (excited with 488nm laser and emission was collected with a band pass filter 525/50 nm) were applied for DAPI and FAM (with excitation/emission maximum at 492/518 nm) signals, respectively.

2.6. Flow Cytometry

For the flow cytometry experiments, the cells were washed twice with phosphate-buffered saline (PBS) and harvested by trypsinization. The FAM served as the luminescent marker (filter set for FITC was applied) to determine the transfection efficiency quantitatively. The samples were analyzed using a FACSCalibur flow cytometer (Becton Dickinson, Mississauga, CA).

2.7. Gene expression analysis

Forty-eight hours after transfection, total RNA was extracted from MIAPaCa-2 cells using E.Z.N.AtM Total RNA Kit (OMEGA) and the amount was quantitated by a spectrophotometer (Nano-Drop ND-1000). Reverse transcription was conducted in a 20 μl reaction mixture and cDNA was synthesized from 2μg of total RNA using the reverse transcriptase kit (Promega) according to the previous experience[28]. The K-ras relative mRNA expression level was determined using Semi-quantitative PCR normalized to the expression of Glyceraldehyde-3-phosphate dehydrogenase (GAPDH), one of the most commonly used housekeeping genes adopted in comparisons of gene expression. According to the previous report[27], the primer sequences for different genes were as follows: K-Ras, forwards 5′-AGAGTGCCTTGACGATACAGC-3′ and reverse 5′-ACAAAGAAAGCCCTCCCCAGT-3′; GAPDH,forwards 5′-ACCACAGTCCATGCCATCAC-3′ and reverse 5′-TCCACCACCCT-GTTGCTGTA-3′. The PCR products were electrophoresed on 1.2% ethidium bromide-stained agarose gel and observed under a UV transilluminator (Bio-Rad).

2.8. Cell proliferation, apoptosis, Migration and invasion Assays

The effect of BCPV-siRNA on the MiaPaCa-2 cell proliferation was detected by MTT assay as **1.3** described above. Wound-healing assay was conducted to examine the capacity of cell migration. The wound-healing assay was conducted as described previously [29, 30]. Briefly, MiaPaCa-2 cells (1×10^4) were seeded into 24-well plates, then transfected with BCPV-siRNA(weight ratio is 8:1) for 48h, in which the cells reached almost confluent. The wound was generated by scratching the surface of the plates with a sterile middle pipette tip. Then, the cells were incubated in complete culture medium and photographed with a Nikon Eclipse-Ti microscope. Cellular migration toward the scratched area was respectively assessed at 0, 24, 48, and 72h (0h is time of scratching line). The distances of migration from the cellular monolayer to the wounded area during this time period was measured by NIS Elements Br Analysis 4.0 software.

The invasive capacity of MiaPaCa-2 cells treated with siRNA transfection or after different treatments were tested by using 8.0-um BD BioCoat Matrigel invasion chambers Assay System (BD Biosciences) according to the manufacturer's protocol with minor modification. Briefly, MiaPaCa-2 cells were transfected with BCPV-siRNA for 48h as described above. Furthermore, the transfected MiaPaCa-2 cells (5×10^4) with free FBS medium were seeded into the upper chamber of the system. Bottom chamber in the system were filled with 10% FBS medium as a chemoattractant. After 48 h of incubation, the cells in the upper chamber were removed with swabs, and the cells that invaded through the Matrigel matrix membrane were stained with 1% crystal violet in PBS buffered saline for 30 minutes. Then, the invaded cells were viewed under the microscope, and counted in 5 random fields of vision.

The apoptosis assay was conducted by FITC Annexin V Apoptosis Detection Kit I (BD PharmingenTM) according to the manufacturer. Briefly, approximately 1×10^6 MiaPaCa-2 cells were seeded in six-well plate. Then, the cells were treated with the BCPV-siRNA (the weight ratio is 8:1) for 72 hours. The cells were then collected and washed twice with cold PBS and suspended in Binding Buffer. Subsequently, the externalization of phosphatidylserine was measured as FITC labeled AnnexinV. The cell nucleus was stained with PI. The stained cells were analyzed by flow cytometry to determine the apoptosis cells.

2.9. Statistical analysis

Data are presented as mean ± SD. Statistical analysis was performed using analysis of variance (ANOVA). All statistical calculations were performed with the SPSS 11.0 software package. When two comparisons were obtained, Student's unpaired two-tailed t test was used. A P value less than 0.01 is regarded as statistically significant.

3. Results and discussion

The BCPVs have been demonstrated as highly efficient carriers for gene delivery[26, 27, 31], especially when serving as siRNA carriers for intracellular delivery, and the schematic drawing of their chemical structure is shown in **Figure 1A**. Since the pore size of the glomerular filtration barrier in the kidney is about 8nm, naked siRNAs can pass through and escape into the nascent urine and be eliminated[32, 33]. As a result, siRNA conjugated nanoparticles should have a proper size of larger than 20 nm to avoid fast renal clearance[34]. The BCPV is a degradable vector with high surface charge (+62.68±9.46mV) for effective siRNA conjugation. Before forming the nanoplexes with siRNAs, the hydrodynamic diameter of BCPV is measured to be 13.64±4.96nm. Prior to further applications, the intrinsic cytotoxicity of the nanoparticles was evaluated through MTT assay on MiaPaCa-2 cells. As shown in **Figure 1B**, over 90% of cells were viable across a large dosage range (up to 160 μg/mL) after 24 or 48h of treatment, indicating that the BCPVs are highly biocompatible.

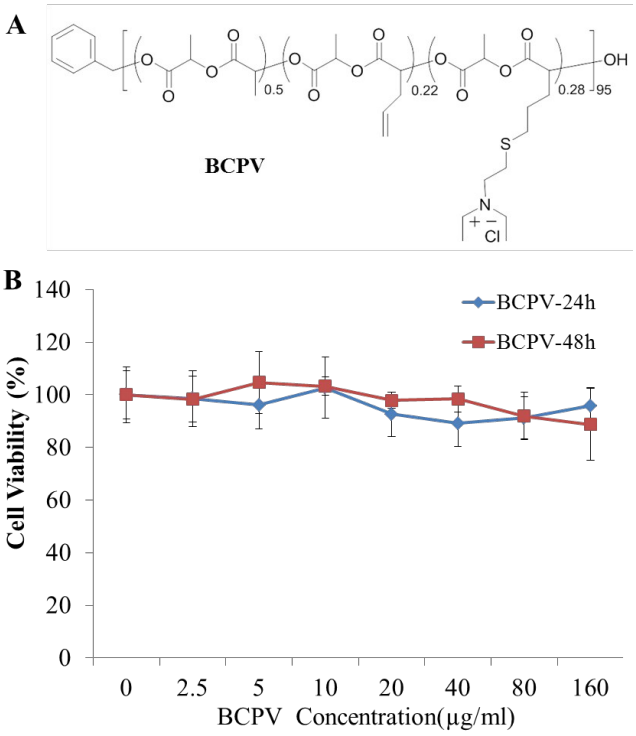

Figure 1. (A) The structure of BCPV reference to the previous reported[26]. (B) Cell viability of MiaPaCa-2 cells treated with BCPV at different concentrations for 24 and 48 hours. Results are represented as means ±SD, n=6.

For efficient delivery, the ratio between the siRNAs and the carriers is an important parameter to optimize. In this study, five different weight ratios (BCPV:siRNA), 1:1, 2:1, 4:1, 8:1 and 16:1 were evaluated, where the weight of siRNA molecules is fixed at 1.25μg. The conjugation of siRNAs to the BCPV was identified by gel electrophoresis. Equal amount of siRNAs were mixed with BCPV at different weight ratios and loaded into a gel electrophoresis. In this process as shown in **Figure 2A**, the bright color associated with the ethidium bromide indicates that the siRNAs conjugated with BCPV were retained in the loading wells while the un-bounded siRNAs migrated to the opposite electrode. As comparing with the pure siRNA channel, decreasing fluorescent intensities could be observed as the ratio of BCPV gets higher. When ethidium bromide is bound to a nucleic acid, its intensity will be amplified. In the cases of high BCPV:siRNA ratio, the excess amount of BCPV "buried" the siRNA and impeded the contact to ethidium bromide, which resulted in decreasing intensities. Nevertheless, it can serve as a clear indication of the siRNA-BCPV conjugation. Also, we found that the BCPV formulation is able to retard for most of the siRNA when the BCPV-siRNA weight ratio is above 8:1. At 8:1 feeding ratio, the BCPV weight is estimated to be 10.25 μg, and siRNA weight is 1.25 μg. Based on these values, the drug loading content is calculated and it is about 11.1 wt% at 8:1 feeding ratio. The hydrodynamic size and zeta potential of the five conjugates were also monitored. As shown in **Fig. 2B**, when siRNAs are conjugated, the size of the nanoplexes has increased to 56.73±20.62nm, 93.69±24.06nm, 84.02±23.59nm, 74.14±25.48nm and 73.95±27.38nm for weight ratios (BCPV:siRNA) of 1:1, 2:1, 4:1, 8:1 and 16:1, respectively. The change in the zeta potential is more obvious. A clear drop in the zeta potential of the positively charge BCPV is identified upon loading of siRNAs. As the ratio of siRNAs gets higher, a constant decrease in the zeta potential is observed due to higher loading ratio of the negatively charged siRNAs.

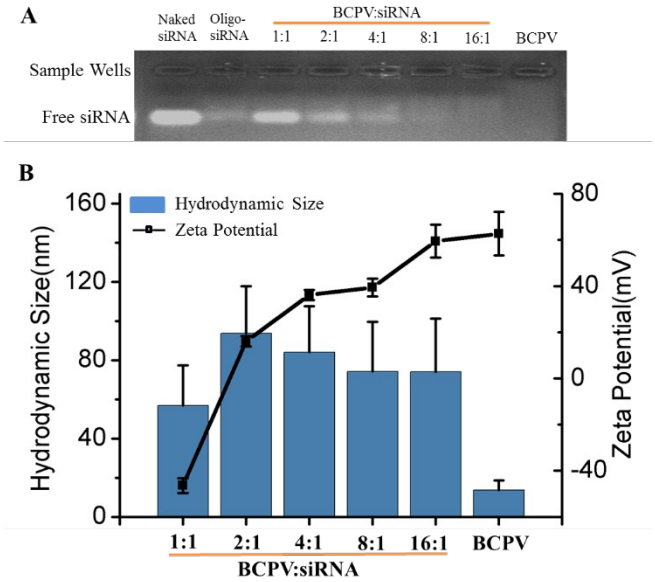

Figure 2. (A) Agarose gel electrophoresis of BCPV/siRNA nanoplexes, Oligo-siRNA as a positive control group. (B) Monitoring of the change in particle hydrodynamic size and zeta potential with different weigh ratios of BCPV:siRNA.

After characterization, BCPV-siRNA complex of different weight ratios were used for cellular transfection, where the weight of siRNA is fixed at 2.5μg. **Figure 3** shows the color coded fluorescence images of MiaPaCa-2 cells treated with different formulations at 4 hour post treatment. The siRNAs were labeled with fluorescent FAM and the signals were rendered in green while the cell nucleus were stained with DAPI and color coded in blue. To obtain a positive control, a commercialized siRNA transfection reagent Oligofectamine™ was introduced (Oligo-siRNA). As shown in Fig. 3, in the cells treated with free siRNAs of same dosage and BCPV alone, no FAM signal was observed (**Figure 3a-c**). As a

comparison, bright FAM signals could be observed in the cells treated with BCPV-siRNA formulations of different weight ratios from 2:1 to 16:1 (**Figure 3e-h**). This demonstrated that BCPV has successfully delivered siRNAs into the cells without rapid degradation. A closer examination could find slight differences on the fluorescence intensities in the BCPV-siRNA groups of various weight ratios. As the weight ratio of BCPVs gets higher, more intense fluorescence could be noted, indicating higher siRNA delivery efficiency. When the weight ratio increases to 8:1, comparable fluorescence intensities could be found between the BCPV-siRNA formulation and the positive control of Oligo-siRNA **(Figure 3d)**.

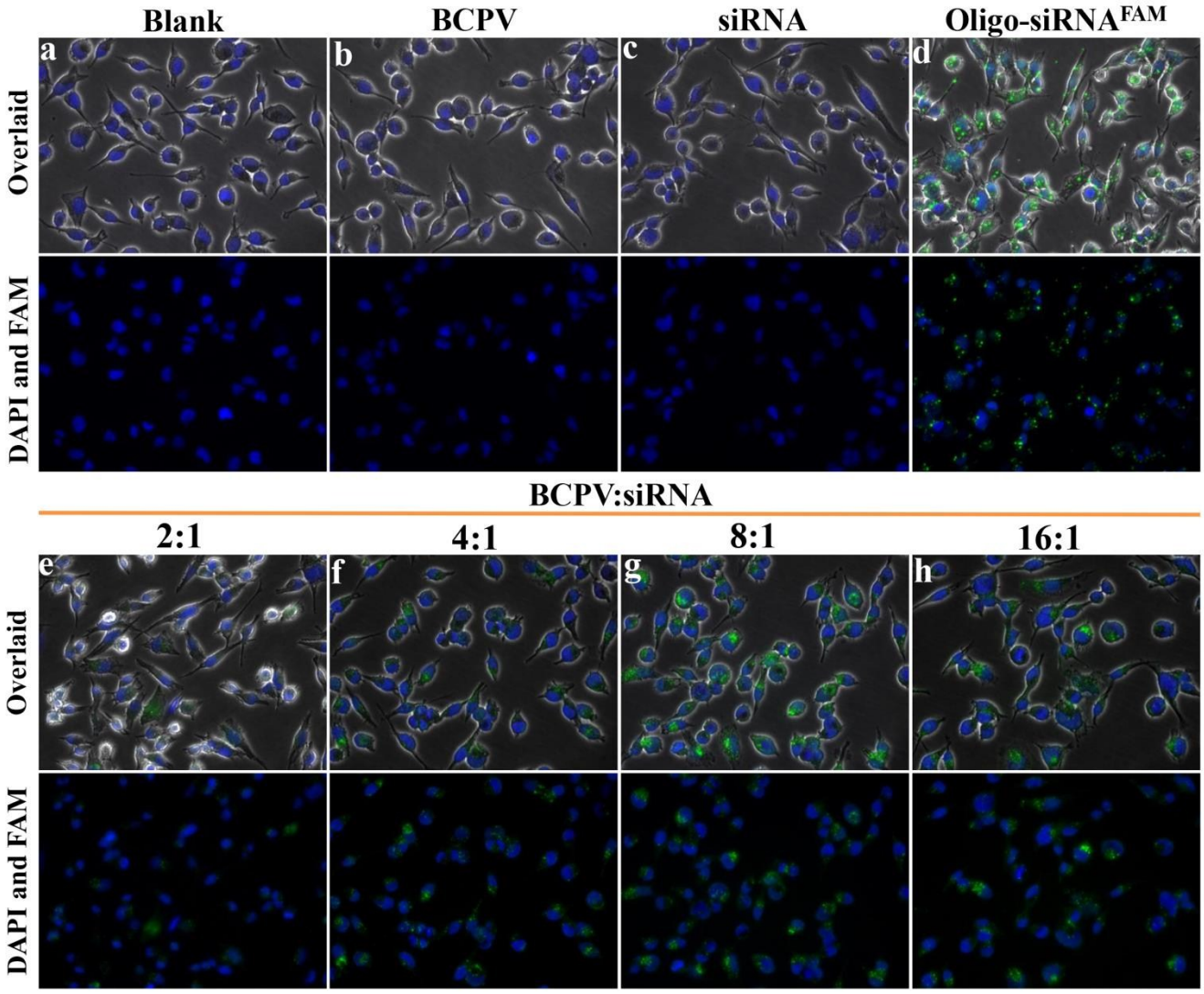

Figure 3. Fluorescence microscopy images of MiaPaCa-2 cells treated with different materials. Cell nucleus are stained with DAPI and rendered in blue, and the fluorescent signal from the FAM labeled siRNA is rendered in green.

To further quantify the transfection efficiency of siRNAs by BCPV, flow cytometry analysis was used and the results were shown in **Figure 4**. For all the treatment groups, a reference gate was chosen to identify the normal cell events (Figure 4a). Based on the intensity of the fluorescent signals, all the gated events were divided into two populations of M1 and M2 (Figure 4b-h), where cells in M1 have low fluorescent signals from autofluorescence while cells in M2 express strong fluorescence from the FAM label. The transfection efficiency was defined as the fraction of M2 which is normalized by the total gated events. Figure 4i summarizes the statistical results from the flow cytometry. It shows that the cells treated with free BCPV(1.05±0.73%) and naked siRNA^{FAM} (2.14±0.63%) have negligible fluorescent signals which are similar to the blank control (0.35 ± 0.01%). For comparison, the cells treated with BCPV-siRNA^{FAM} have shown remarkably high transfection efficiencies of 96.69±1.16%, 96.52±1.40%, and 96.15±2.19%, for weight ratio of 4:1, 8:1 and 16:1, respectively, which are comparable with the positive control group Oligo-siRNA (84.95±3.90%). In addition to the transfection efficiency, the average fluorescent intensity was also recorded, which indicates the averaged siRNAs delivery efficiency to cells. The result shows that although different weight ratios of BCPV share similar transfection

efficiency with the positive control, the averaged siRNAs delivery efficiency varies for different BCPVs ratios. Since the siRNA loading capacity per BCPV is limited, there were excess amount of free siRNAs in the 4:1 group left unconjugated, which will eventually be dissipated during the transfection process. Increasing the weight ratio of BCPVs leads to a higher concentration of the effective transfection complex BCPV-siRNA. As a result, the 8:1 group shows a higher average fluorescent intensity than the 4:1 group. However further increase of the BCPVs weight ratio results in an insufficient siRNA loading per nanoparticle and consequently there is no significant difference in the overall average fluorescent intensity between the 8:1 and 16:1 groups.

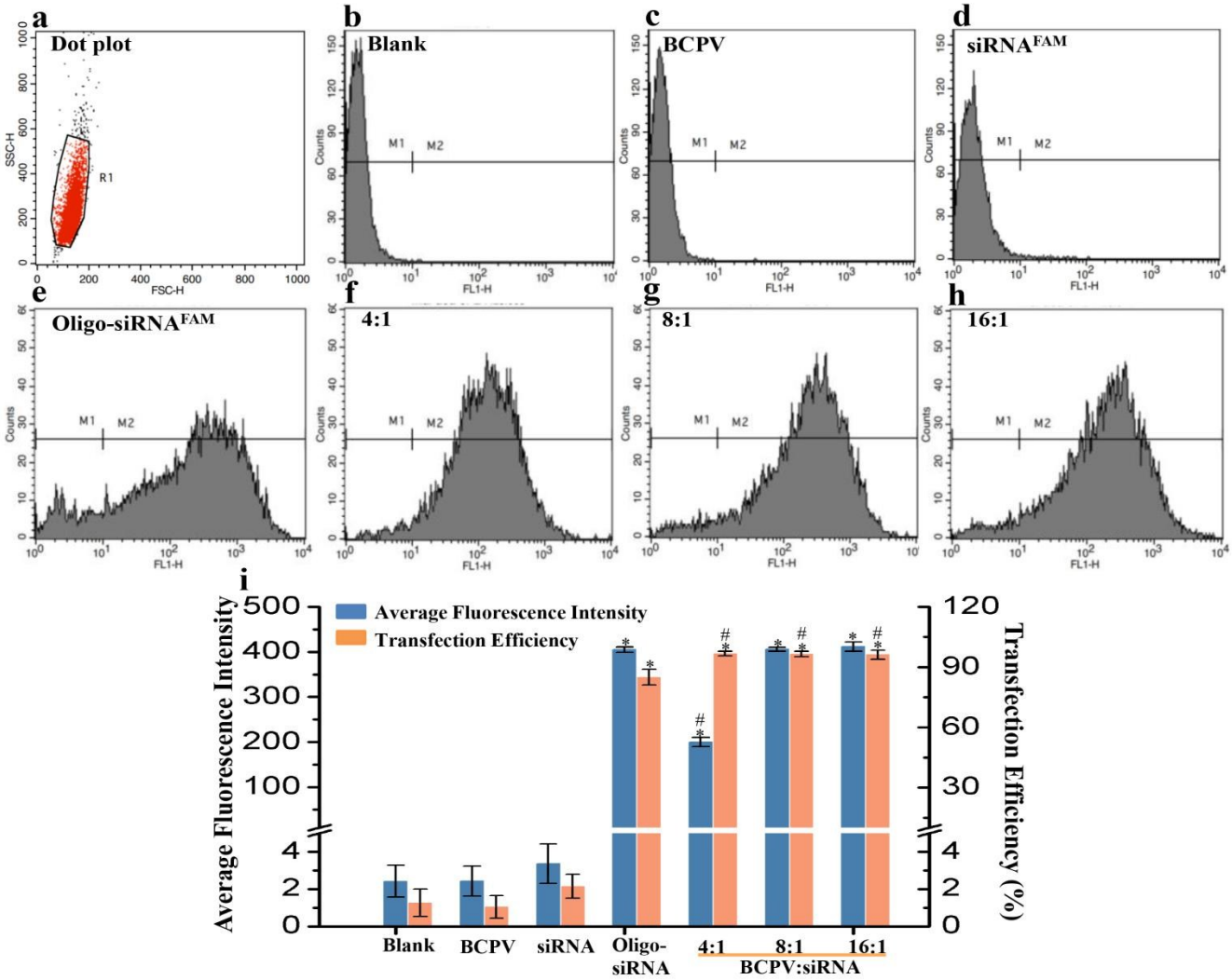

Figure 4. Transfection efficiency of MiaPaCa-2 cells evaluated by flow cytometry. (a) Dot plot of cells, the cells in the R1 region were selected for evaluating the transfection efficiency, (b)~(h) are statistical count of cells treated with PBS, BCPV, siRNA^{FAM}, Oligo-siRNA^{FAM}, and BCPV/siRNA^{FAM} at different weight ratio of 4:1, 8:1 and 16:1, respectively. Accordingly, the concentrations of BCPV are estimated to be 10 μg/ml, 20 μg/ml and 40 μg/ml where the weight ratios of BCPV-siRNA complexes are determined to be 4:1, 8:1 and 16:1. (i) Quantitative evaluation of the results from (b)~(h) showing the average fluorescent intensity and transfection efficiency of each group. Average fluorescence intensity presents the FAM intensity in the cells. The transfection efficiency is defined as the ratio between the cell counts of M2 (transfected cell counts) to M1+M2 (total cell counts). The relative values shown are means ±SD, n=3 (*, P<0.01 compared to Blank group, #,P<0.01 compared to Oligo-siRNA group).

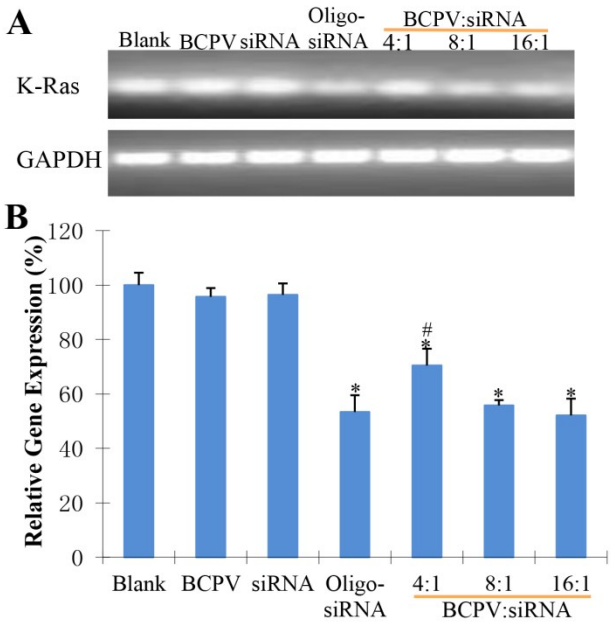

Figure 5. Gene expression of K-ras in MiaPaCa-2 cells of different treatment groups. (A) Agarose gel electrophoresis of K-ras relative expression. (B) Quantitative relative gene expression of K-ras after siRNA transfection of different treatment groups. The relative values shown are means ±SD, n=3 (*, P<0.01 compared to Blank group. #, P<0.01 compared to Oligo-siRNA group).

To verify the knockdown efficiency by different formulations, the expression of mutated K-ras gene was evaluated at the mRNA level through the agarose gel electrophoresis. Using the housekeeping gene GAPDH as reference, the mRNA levels of the mutant K-ras gene from different treatment groups were extracted and normalized to the control group. As shown in **Figure 5**, the relative gene expression of mutant K-ras of the BCPV treated group and the free siRNA treated group share no obvious difference with the blank control. In contrast, the BCPV-siRNA treated groups have shown significant knockdown efficiencies. Specifically, the groups with weight ratio of 8:1 and 16:1 have shown comparable knockdown efficiencies of 44.24±2.01% and 47.85±6.11%, respectively, with the Oligo-siRNA treated positive control group (46.67±6.23%), while the 4:1 weight ratio group has a slightly lower knockdown efficiency of 29.56±6.16%. This is because there were also unconjugated free siRNAin the 4:1 weight ratio group as mentioned earlier. According to these results, a BCPV:siRNA weight ratio of 8:1 can significantly inhibit the mutant K-ras gene expression in MiaPaCa-2 cells and this ratio will be used in the following experiments.

The monomeric ras family G proteins act as "molecular switches" linking extracelluar signals to intracellular signals through membrane receptors. As GTPases, they cycle from a GDP-bound "off" state to a GTP-bound "on" state in response to the activation from various receptors. Activated ras targets a number of downstream effectors including Raf kinase, Phosphoinositide 3'-kinase (PI3-K) and RalGEFs to produce pleiotropic cellular effects that affect cell growth, differentiation and survival[35]. The point mutation at codon 12 in the K-ras gene reduces the intrinsic GTPase activity of the protein and lock the protein to the GTP-bound "on" state, which leads to constitutive activation and eventually cancer progression[36, 37]. The inhibition of the mutant K-ras expression has been reported to promote cell apoptosis[4, 6, 38, 39] and also to inhibit cell proliferation[40, 41], migration[30] and invasion[7]. In this study, the cellular activities of MiaPaCa-2 cells were systematically evaluated after the mutant K-ras gene transfection by BCPV-siRNA complex.

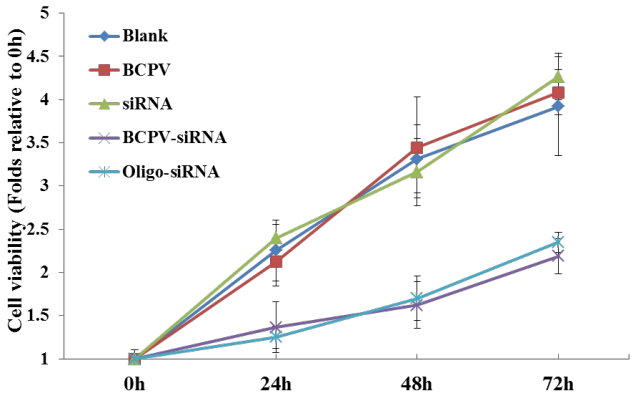

Figure 6. Proliferation of MiaPaCa-2 cells after treatment with different formulations. Cells were first treated with BCPV, siRNA, BCPV-siRNA and Oligo-siRNA, then continued to culture for 24h, 48h, and 72h. Cell viability was determined using MTT cell viability assay. Results are represented as means ±SD, n=3.

Figure 6 shows the proliferation of MiaPaCa-2 cells after treating with different formulations. The BCPVs as well as the free siRNA treated groups have shown the similar trends with the blank control group where the cell population doubled after 24 hours and proliferated to 4 folds after 72 hours. In contrast, after the treatment with BCPV-siRNA, a significant inhibition in the cell proliferation could be observed. The proliferation rate has been greatly altered by the successful delivery of siRNAs. In addition to the cell proliferation evaluation, the migration of the cells after treatments was also assessed. As shown in **Figure 7A**, a scratch wound in the monolayer cell culture of MiaPaCa-2 cells was generated for each of the different treatment groups. In the non-treated blank group, a decrease in the window width could be clearly observed after 24 hours. At 48 hour post treatment, the cells started to migrate to the open space in between the wound margins as the window closes further and the previously straight wound boundaries become cluttered. After 72 hours, the wound has almost completely healed and the boundaries are hardly identified. Similar observations could be found in the BCPVs and free siRNA treated groups. As a comparison, a significantly suppressed healing process is observed in the cells treated with the BCPV-siRNA complex or Oligo-siRNA. The decrease of the window width is much slower than those in the other groups. More importantly, it took the cells 72 h to migrate to the open space in between the wound boundaries. It is reported that the wound healing process in cell culture is caused by a combination of proliferation and migration of cells in response to the disruption of cell-cell contacts and an increased concentration of growth factors[42, 43]. It is a commonly used method to study the cell migration and the underlying biology[44, 45]. As shown in **Figure 7B**, the healing

process of each group is further quantified and expressed as the normalized percentage of the wound closure. It clearly shows the difference between the BCPV-siRNA treated group and the other three groups, where the wound in the BCPV-siRNA treated group closes at almost a half-speed as the other three groups. These results indicate that the gene expression regulation of mutant K-ras in MiaPaCa-2 cells mediated by the BCPV-siRNA complex have successfully changed the expression pattern of the downstream gene associated with the cell proliferation and migration. Moreover, there is no significant difference was observed among the BCPV-siRNA and Oligo-siRNA group. Cell migration is a complex process which can be viewed as a process regulate my matrix-degrading proteinases, integrins and other cell adhesion molecules[46]. It is a critical event in cancer progression and especially metastasis[47]. The inhibition of the cell migration by silencing the mutant K-ras gene in MiaPaCa-2 cells has provided a potential therapeutic way for the treatment of pancreatic cancer.

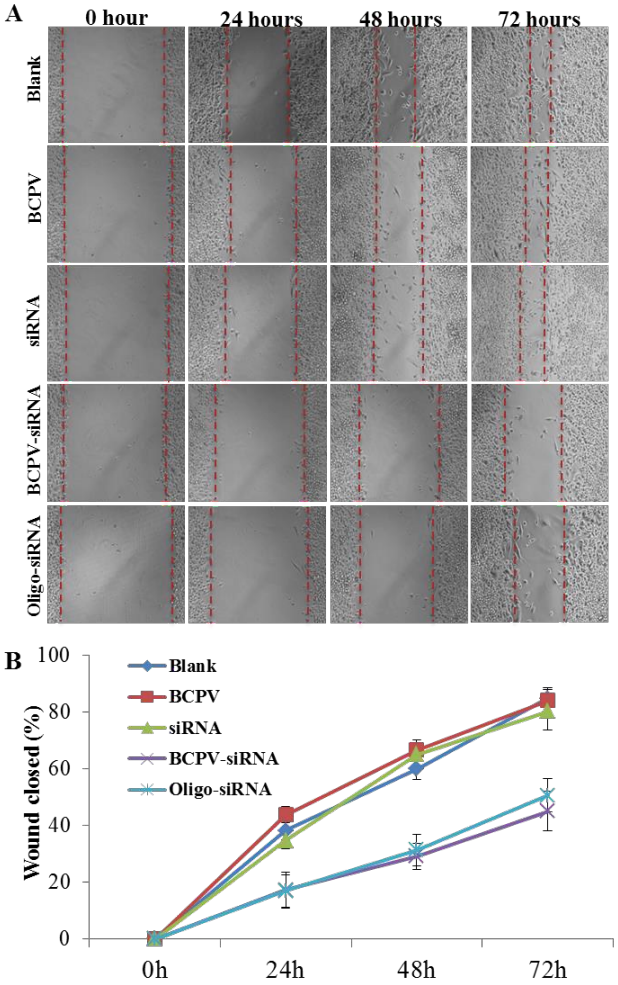

Figure 7. Wound healing assay in MiaPaCa-2 cell culture treated with different formulations. (A) Phase contrast microscope images of the wound healing process monitored for 72 hours post treatment. (B) Quantitative evaluation on the percentage of window close after treatment, values were normalized by the initial wound window width.

Metastatic tumor spreading to distant different organs is the primary cause of death in pancreatic cancer. Metastasis is a complex and multi-step process which starts with the migration and invasion of primary tumor cells to the adjacent tissue[48, 49]. As a result, the ability to block the migratory and invasive capacity of cancer cells is a main approach to treat patients with malignant cancer[50, 51]. To assess the change in the invasion capacity of MiaPaCa-2 cells treated by different formulations, an *in vitro* Matrigel invasion chambers assay was conducted[52, 53]. The main component laminin and type IV collagen of Matrigel has provided it the structural and biochemical properties of basement membranes[54]. The capability of cells penetrating through the membrane is a good measurement of their invasiveness and metastatic potential[55]. As shown in **Figure 8**, the population of penetrated cells from the BCPV-siRNA and Oligo-siRNA treated group is significantly smaller than those of the other three control groups. In the quantitative measurement, the normalized data shows that the cells able to penetrate through the Matrigel in the BCPV-siRNA treated group is over 60% less than the blank control group. These results clearly suggest that the knockdown of K-ras by BCPV-siRNA but not free siRNAs could retard the invasion and subsequently the metastasis of pancreatic cancer cells.

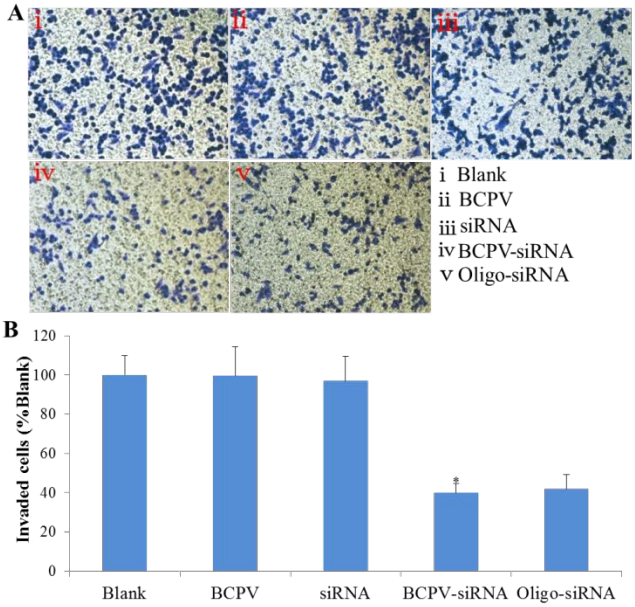

Figure 8. Cell invasion assay based on a transwell chamber model of MiaPaCa cells after treatment with different formulations. (A) Bright field microscope images of cells that penetrated through the Matrigel-coated membrane in the transwell chammber. Cells were stained with trypan blue. (B) Quantitative cell counts on the cells penetrated through the Matrigel-coated membrane. Each bar represents five random microscopic fields under 20× magnification. Error bar indicate SD, *P<0.01 compared with Blank group, n=5.

Finally, the apoptosis of MiaPaCa-2 cells treated with different formulations were assessed by FITC labeled annexin V and propidium iodide (PI) staining. Annexin V has a high affinity for the membrane phospholipid phosphatidylserine (PS), which is exposed to the external cellular environment in apoptotic cells. It has been widely used as an early apoptosis indicator. PI is a vital dye which will be excluded by viable cells with intact membranes. It is commonly used to label the dead and damaged cells. As shown in

Figure 9, after 72 hours treatment, the FITC and PI positive apoptotic cell counts in the Q2 zone of the BCPV-siRNA treated group show a conspicuous difference with the other three groups. The quantitative data indicates no significant difference between the blank control group (17.19±2.72%) and BCPV (16.11±2.79%) or free siRNAs (17.47±2.44%) treated groups, while the apoptotic cell population in the BCPV-siRNA treated group is doubled (37.52±3.15%). When compare to the Oligo-siRNA group (32.67±4.11%), no statistically significant differences are observed for the BCPV-siRNA group.

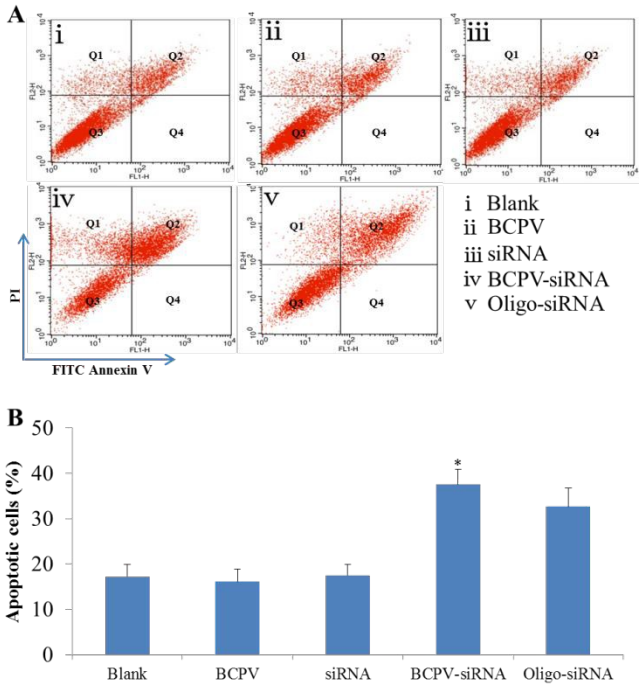

Figure 9. FITC Annexin V and Propidium Iodide (PI) co-stained apoptosis assay on MiaPaCa-2 cells treated with different formulations (Blank, BCPV only, siRNA only and BCPV-siRNA) at 72 h post-treatment. (A) Apoptotic cells stained with Annexin V/PI were measured by flow cytometry. (B) Late apoptotic cell counts in the upper right quadrant (Q2) of different treatment groups. Error bar indicate SD, *P<0.01 compared with Blank group, n=5.

To date, cancer therapy has entered a stage of personalized treatment where targeted gene therapy is regarded as the most promising choice. As the K-ras mutation mainly occurs in the early phase of pancreatic ductal carcinogenesis, the knockdown of the mutated K-ras gene at the early stage of pancreatic cancer is of vital importance. However, the efficiency of knockdown largely depends on the selection of proper carriers. Our findings demonstrated that the inactivation of mutated K-ras gene by BCPV-siRNA leads to a significant inhibition of cellular proliferation, migration, invasion and anti-apoptosis in MiaPaCa-2 cells. To the best of our knowledge, this is the first report that demonstrates the comprehensive effects of K-ras gene knockdown on pancreatic cancer cells mediated by biocompatible and biodegradable nanoparticle conjugated siRNAs. According to such results, the BCPV-siRNA delivery system is far-reaching in gene therapy for pancreatic cancer, which successfully overcomes some challenges in RNA interference and will serve as a promising candidate for gene therapy in pancreatic cancer treatment. Yet it is also worth noting that before entering into clinics, the stability in the bloodstream, immunotoxicity, and metabolic pathways of BCPV-siRNA in vivo still need to be carefully evaluated and its therapeutic effect in animal tumor models also needs to be assessed.

4. Conclusion

In conclusion, we have demonstrated the use of a biocompatible and biodegradable cationic polymer based nanoparticle formulation for the delivery of siRNAs targeting the mutant K-ras oncogene in pancreatic cancer cells. We have shown that the expression of mutant K-ras gene was efficiently suppressed through fluorescent imaging and quantitative flow cytometry assessment. In addition, we have monitored the consequence of the K-ras knock down in the MiaPaCa-2 cells. Results have shown that the RNA interference process have initiated the change in the expression pattern of the downstream gene that regulates the cell proliferation, migration and apoptosis. With an optimized weight ratio between the nanocarriers and siRNAs, we have significantly reduced the growth, migration, invasion of MiaPaCa-2 cells, and the apoptosis of the pancreatic cancer cells has also been promoted. Taken together, these in vitro results have demonstrated the great potential of the BCPV in gene therapy of pancreatic cancer. Although in vivo tests of the nanoparticle formulation are still pending, we envision that it could serve as an excellent nanocarrier platform for genetic materials in clinical settings of gene therapy.

Acknowledgements

The authors are grateful for the original molecular structure design of BCPV from Professor Chong Cheng at University at Buffalo. The study was supported by the Start-up grant (M4080141.040) from Nanyang Technological University, Tier1 Academic Research Funds (M4010360.040 RG29/10) from Singapore Ministry of Education and partially from the Singapore Ministry of Education under Tier 2 Research Grant MOE2010-T2-2-010 (4020020.040 ARC2/11), the grants from National Natural Science Foundation of China (NSFC) (NO. 81301318, 61107017& 81400591), the Start-up grant from the Department of Fiber and Composite Materials at Feng Chia University and the research grant (No. MOST 103-2218-E-035-010) from the Ministry of Science and Technology of Taiwan, Republic of China. The authors also appreciate the Precision Instrument Support Center of Feng Chia University in providing the fabrication and measurement facilities.

References

1. M. A. Collins, J. C. Brisset, Y. Q. Zhang, F. Bednar, J. Pierre, K. A. Heist, C. J. Galban, S. Galban and M. P. di Magliano, *Plos One*, 2012, **7**.
2. R. Siegel, D. Naishadham and A. Jemal, *Ca-a Cancer Journal for Clinicians*, 2012, **62**, 10-29.
3. Y. Li, T. G. VandenBoom, Z. Wang, D. Kong, S. Ali, P. A. Philip and F. H. Sarkar, *Cancer research*, 2010, **70**, 1486-1495.
4. A. Arlt, S. S. Muerkoster and H. Schafer, *Cancer Letters*, 2013, **332**, 346-358.
5. M. Tada, M. Ohashi, Y. Shiratori, T. Okudaira, Y. Komatsu, T. Kawabe, H. Yoshida, R. Machinami, K. Kishi and M. Omata, *Gastroenterology*, 1996, **110**, 227-231.

6. T. Tsuchida, H. Kijima, S. Hori, Y. Oshika, T. Tokunaga, K. Kawai, H. Yamazaki, Y. Ueyama, K. J. Scanlon, N. Tamaoki and M. Nakamura, *Cancer Gene Therapy*, 2000, **7**, 373-383.
7. J. B. Fleming, G. L. Shen, S. E. Holloway, M. Davis and R. A. Brekken, *Molecular Cancer Research*, 2005, **3**, 413-423.
8. G. J. Hannon, *Nature*, 2002, **418**, 244-251.
9. R. Kanasty, J. R. Dorkin, A. Vegas and D. Anderson, *Nature Materials*, 2013, **12**, 967-977.
10. C. Huang, M. Li, C. Y. Chen and Q. Z. Yao, *Expert Opinion on Therapeutic Targets*, 2008, **12**, 637-645.
11. J. Wang, Z. Lu, M. G. Wientjes and J. L. S. Au, *Aaps Journal*, 2010, **12**, 492-503.
12. D. L. Lewis and J. A. Wolff, *Advanced Drug Delivery Reviews*, 2007, **59**, 115-123.
13. F. Petrocca and J. Lieberman, *Journal of Clinical Oncology*, 2011, **29**, 747-754.
14. S. L. Ameres and P. D. Zamore, *Nat Rev Mol Cell Biol*, 2013, **14**, 475-488.
15. C. G. Chen and Z. T. Yu, *Anticancer Research*, 2009, **29**, 1367-1372.
16. Y. H. Zhi, M. M. Song, P. L. Wang, T. Zhang and Z. Y. Yin, *World Journal of Gastroenterology*, 2009, **15**, 1072-1078.
17. J. Guillermet-Guibert, L. Davenne, D. Pchejetski, N. Saint-Laurent, L. Brizuela, C. Guilbeau-Frugier, M. B. Delisle, O. Cuvillier, C. Susini and C. Bousquet, *Molecular Cancer Therapeutics*, 2009, **8**, 809-820.
18. D. Peer and J. Lieberman, *Gene Therapy*, 2011, **18**, 1127-1133.
19. K. A. Whitehead, R. Langer and D. G. Anderson, *Nat Rev Drug Discov*, 2009, **8**, 129-138.
20. A. El-Aneed, *Journal of Controlled Release*, 2004, **94**, 1-14.
21. S. C. Semple, A. Akinc, J. Chen, A. P. Sandhu, B. L. Mui, C. K. Cho, D. W. Y. Sah, D. Stebbing, E. J. Crosley, E. Yaworski, I. M. Hafez, J. R. Dorkin, J. Qin, K. Lam, K. G. Rajeev, K. F. Wong, L. B. Jeffs, L. Nechev, M. L. Eisenhardt, M. Jayaraman, M. Kazem, M. A. Maier, M. Srinivasulu, M. J. Weinstein, Q. Chen, R. Alvarez, S. A. Barros, S. De, S. K. Klimuk, T. Borland, V. Kosovrasti, W. L. Cantley, Y. K. Tam, M. Manoharan, M. A. Ciufolini, M. A. Tracy, A. de Fougerolles, I. MacLachlan, P. R. Cullis, T. D. Madden and M. J. Hope, *Nat Biotech*, 2010, **28**, 172-176.
22. A. Akinc, A. Zumbuehl, M. Goldberg, E. S. Leshchiner, V. Busini, N. Hossain, S. A. Bacallado, D. N. Nguyen, J. Fuller, R. Alvarez, A. Borodovsky, T. Borland, R. Constien, A. de Fougerolles, J. R. Dorkin, K. Narayanannair Jayaprakash, M. Jayaraman, M. John, V. Koteliansky, M. Manoharan, L. Nechev, J. Qin, T. Racie, D. Raitcheva, K. G. Rajeev, D. W. Y. Sah, J. Soutschek, I. Toudjarska, H.-P. Vornlocher, T. S. Zimmermann, R. Langer and D. G. Anderson, *Nat Biotech*, 2008, **26**, 561-569.
23. J. P. Dassie, X.-y. Liu, G. S. Thomas, R. M. Whitaker, K. W. Thiel, K. R. Stockdale, D. K. Meyerholz, A. P. McCaffrey, J. O. McNamara Ii and P. H. Giangrande, *Nat Biotech*, 2009, **27**, 839-846.
24. K. Lappalainen, I. Jaaskelainen, K. Syrjanen, A. Urtti and S. Syrjanen, *Pharmaceutical Research*, 1994, **11**, 1127-1131.
25. G. Lin, C. Yang, R. Hu, C.-K. Chen, W.-C. Law, T. Anderson, B. Zhang, Q. T. Nguyen, H. T. Toh, H. S. Yoon, C. Cheng and K.-T. Yong, *Biomaterials Science*, 2014, **2**, 1007-1015.
26. C. H. Jones, C.-K. Chen, M. Jiang, L. Fang, C. Cheng and B. A. Pfeifer, *Molecular pharmaceutics*, 2013, **10**, 1138-1145.
27. G. Lin, R. Hu, W.-C. Law, C.-K. Chen, Y. Wang, H. Li Chin, Q. T. Nguyen, C. K. Lai, H. S. Yoon, X. Wang, G. Xu, L. Ye, C. Cheng and K.-T. Yong, *Small*, 2013, **9**, 2757-2763.
28. C. B. Yang, X. C. Mo, J. Z. Lv, X. Y. Liu, M. C. Yuan, M. Dong, L. Li, X. P. Luo, X. M. Fan, Z. Jin, Z. G. Liu and J. Liu, *Experimental Physiology*, 2012, **97**, 1315-1327.
29. C. Xu, D.-m. Hu and Q. Zhu, *Clinical & Experimental Metastasis*, 2013, **30**, 933-944.
30. K. Yoshikawa, E. Tanabe, A. Shibata, S. Inoue, M. Kitayoshi, S. Okimoto, N. Fukushima and T. Tsujiuchi, *Experimental Cell Research*, 2013, **319**, 105-112.
31. C. K. Chen, W. C. Law, R. Aalinkeel, B. Nair, A. Kopwitthaya, S. D. Mahajan, J. L. Reynolds, J. Zou, S. A. Schwartz, P. N. Prasad and C. Cheng, *Advanced Healthcare Materials*, 2012, **1**, 751-761.
32. J. Wartiovaara, L. G. Ofverstedt, J. Khoshnoodi, J. J. Zhang, E. Makela, S. Sandin, V. Ruotsalainen, R. H. Cheng, H. Jalanko, U. Skoglund and K. Tryggvason, *Journal of Clinical Investigation*, 2004, **114**, 1475-1483.
33. Y. Y. Huang, J. M. Hong, S. Q. Zheng, Y. Ding, S. T. Guo, H. Y. Zhang, X. Q. Zhang, Q. A. Du and Z. C. Liang, *Molecular Therapy*, 2011, **19**, 381-385.
34. H. Lee, A. K. R. Lytton-Jean, Y. Chen, K. T. Love, A. I. Park, E. D. Karagiannis, A. Sehgal, W. Querbes, C. S. Zurenko, M. Jayaraman, C. G. Peng, K. Charisse, A. Borodovsky, M. Manoharan, J. S. Donahoe, J. Truelove, M. Nahrendorf, R. Langer and D. G. Anderson, *Nat Nano*, 2012, **7**, 389-393.
35. B. B. Friday and A. A. Adjei, *Biochimica Et Biophysica Acta-Reviews on Cancer*, 2005, **1756**, 127-144.
36. D. Lowy and B. Willumsen, *Annual review of biochemistry*, 1993, **62**, 851-891.
37. M. Trahey and F. McCormick, *Science*, 1987, **238**, 542-545.
38. A. Takashima and D. V. Faller, *Expert Opinion on Therapeutic Targets*, 2013, **17**, 507-531.
39. P. Jasinski, P. Zwolak, K. Terai and A. Z. Dudek, *Translational research : the journal of laboratory and clinical medicine*, 2008, **152**, 203-212.
40. Y. Miura, S. Ohnami, K. Yoshida, M. Ohashi, M. Nakano, S. Ohnami, M. Fukuhara, K. Yanagi, A. Matsushita, E. Uchida, M. Asaka, T. Yoshida and K. Aoki, *Cancer Letters*, 2005, **218**, 53-62.
41. T. R. Brummelkamp, R. Bernards and R. Agami, *Cancer Cell*, 2002, **2**, 243-247.
42. B. L. Coomber and A. I. Gotlieb, *Arteriosclerosis, Thrombosis, and Vascular Biology*, 1990, **10**, 215-222.
43. J.-M. Zahm, H. Kaplan, A.-L. Hérard, F. Doriot, D. Pierrot, P. Somelette and E. Puchelle, *Cell motility and the cytoskeleton*, 1997, **37**, 33-43.
44. M. G. Lampugnani, in *Adhesion Protein Protocols*, Springer, 1999, pp. 177-182.
45. J. C. Yarrow, Z. E. Perlman, N. J. Westwood and T. J. Mitchison, *BMC biotechnology*, 2004, **4**, 21.
46. H. A. Chapman, *Current Opinion in Cell Biology*, 1997, **9**, 714-724.
47. M. Björklund and E. Koivunen, *Biochimica et Biophysica Acta (BBA) - Reviews on Cancer*, 2005, **1755**, 37-69.
48. I. J. Fidler, *Nat Rev Cancer*, 2003, **3**, 453-458.
49. L. A. Liotta, *Cancer Research*, 1986, **46**, 1-7.
50. J. D. Hood and D. A. Cheresh, *Nat Rev Cancer*, 2002, **2**, 91-100.
51. P. Friedl and K. Wolf, *Nat Rev Cancer*, 2003, **3**, 362-374.
52. A. Valster, N. L. Tran, M. Nakada, M. E. Berens, A. Y. Chan and M. Symons, *Methods*, 2005, **37**, 208-215.
53. A. Lal, C. A. Glazer, H. M. Martinson, H. S. Friedman, G. E. Archer, J. H. Sampson and G. J. Riggins, *Cancer Research*, 2002, **62**, 3335-3339.
54. H. K. Kleinman, M. L. McGarvey, J. R. Hassell, V. L. Star, F. B. Cannon, G. W. Laurie and G. R. Martin, *Biochemistry*, 1986, **25**, 312-318.
55. H. Kobayashi, H. Ohi, M. Sugimura, H. Shinohara, T. Fujii and T. Terao, *Cancer Research*, 1992, **52**, 3610-3614.